Program Digest, 2019 IEEE International Ultrasonics Symposium (IUS)
Glasgow, Scotland, October 6-9, 2019

A Time-Frequency Independent Component Analysis Method for Group Velocity Extraction of Ultrasonic Guided Waves

Sijia Lou[1], Kailiang Xu*[1, 2], Xue Jiang[1, 2], Bo Hu[1], Lawrence H. Le[3], Dean Ta[1, 2]
[1] Department of Electronic Engineering, Fudan University, Shanghai, 200433, China.
[2] Zhuhai Fudan Innovation Institute, Zhuhai, Guangdong, 519000, China.
[3] Department of Radiology and Diagnostic Imaging, University of Alberta, Edmonton, AB, T6G2R3, Canada.

Abstract—**Ultrasonic guided waves play an important role in non-destructive evaluation (NDE). Nevertheless, the multi-mode dispersion still brings challenges for mode identification and the waveguide evaluation. In this study, we propose a multimodal separation method combining short-time Fourier transform (STFT) with independent component analysis (ICA). The simulation result shows that this method can realize an automatic mode identification and group velocity extraction, which can be helpful in the waveguide assessment.**

Keywords—Multimodal separation, Time-frequency energy ridge, Group velocity extraction, Waveguide evaluation.

I. Introduction

Ultrasonic guided waves have been widely used for non-destructive evaluation (NDE) [1]. However, due to the mode conversion and dispersion, the received signal usually contains multiple modes, which brings challenges for mode identification and waveguide evaluation.

The time-frequency representation (TFR) method has been widely applied to analyze the dispersion characteristic of the ultrasonic guided waves. The technique projects the temporal signals into the time-frequency domain, thus allowing the component of each mode be identified as individual time-frequency trajectory. A considerable number of signal processing methods have been proposed to extract the single mode components from multimodal guided signals. Xu *et al.* [2] introduced the so-called Crazy-Climber method into the signal processing of ultrasonic guided waves, which allows to separate time-frequency ridges of individual modes from TFR of multimodal signals. The Crazy-Climber method has been applied to analyze the guided waves in the long bone [3]. Zoubi *et al.* [4] applied the Crazy-Climber method for mode separation and anomaly imaging. Yang *et al.* [5] used a generalized warblet transform to improve the energy concentration in the time-frequency domain. Zhang *et al.* [6] combined the time-frequency energy distribution with image segmentation technology to realize multimodal guided waves separation. Liu *et al.* [7] introduced synchrosqueezed wavelet transform (SWT) to increase the resolution of time-frequency energy representation. He *et al.* [8] applied the time-reassigned synchrosqueezing transform (TSST) to impulse-like signals, which promotes the energy concentration in the time direction specifically.

Other than the TFR method, some other mode extraction methods have been introduced. Radon transform can be used to project the array signals into the slowness-time domain, so that different mode components can be identified according to different slowness [9-11]. Xu *et al.* [12] proposed a dispersion compensation based mode separation method. With the known dispersion curves, the desired mode can be compensated into a pulse and can thus be separated using a temporal window. Dispersive Radon transform [13], which can map the multichannel dispersive signals of each individual mode into a well localized region in the dispersive Radon domain, provides an efficient solution for mode identification and extraction. Based on the sparsity of the dispersion curves in the frequency-wavenumber domain, Gao *et al.* [14] employed compressed sensing to separate mode superposition.

Different from the previous studies of time-frequency analysis based guided mode separation, instead of applying the time-frequency ridges extraction, we intend to combine STFT with independent component analysis (ICA) for realizing an automatic multimodal separation and group velocity extraction. Assuming that the received signal is a summation of independent non-Gaussian signals, ICA is a useful tool for blind source separation. It has been widely applied to mixed signal processing, such as speaker verification [15], electroencephalographic (EEG) source localization [16], communication systems [17], and fault analysis [18].

In this paper, a finite-difference time-domain (FDTD) simulation is used to obtain the multimodal simulated signals with different incident angles. The temporal signals are mapped into time-frequency domain using STFT method. ICA is used to separate the independent components afterwards. After mode separation, the frequency-dependent group velocity of each mode is further acquired.

II. Materials and Methods

A. Short Time Fourier Transform

The classical STFT [19] is employed to obtain the time-frequency distribution of the guided wave signals. For a given signal $x_i(t)$, it is expressed as follows:

$$x_i(t,f)=\int_{-\infty}^{+\infty} x_i(\tau)\mathrm{g}(\tau\text{-}t)\exp(\text{-}j2\pi f\tau)\mathrm{d}\tau, \qquad (1)$$

This work was supported by the National Natural Science Foundation (11525416, 11974081, 11827808 and 11604054), Natural Science Foundation of Shanghai (19ZR1402700), Shanghai Municipal Science and Technology Major Project (2017SHZDZX01) and State Key Laboratory of ASIC and System Project (2018MS004). Corresponding author: Kailiang Xu, xukl@fudan.edu.cn.

where g(τ-t) is a window function with t as its center. In this research, Gaussian window function is used. The window length is set as 1/20 of that of the temporal signal. The inverse STFT can also be applied to transform the $x_i(t,f)$ backward to the $x_i(t)$.

B. Independent Component Analysis

After STFT, the ICA method is used to achieve the independent component separation. In order to simplify the calculation, preprocessing methods, including de-average and whitening, are usually employed before ICA.

The time-frequency distribution of a signal is assumed to be a linear superposition of multiple independent modes:

$$\mathbf{X}=\mathbf{AS}, \tag{2}$$

where **X** and **S** denote the matrix of received signals and independent components respectively, and **A** is the coefficient matrix. What should be paid attention to is that at least n observations are needed to recover n independent modes from the mixture. The variables in **X** have zero mean and unit variance, which can be guaranteed through de-average and whitening. The main idea of ICA is to seek the optimal representation of the matrix **W** to estimate **S**:

$$\mathbf{Y}=\bar{\mathbf{S}}=\mathbf{WX}. \tag{3}$$

Through approximations of negentropy, fast ICA [20] transforms the mutual information minimization problem into an optimization problem:

$$\text{maximize } \mathrm{J}(\mathrm{w}_i)=\textstyle\sum_{i=1}^{n}[\mathrm{E}\{\mathrm{G}(\mathrm{w}_i^{\mathrm{T}}\mathrm{x}_i)\}-\mathrm{E}\{\mathrm{G}(\mathrm{v})\}]^2, \tag{4}$$

where n equals the number of independent components in **S**, w_i and x_i are variables in **W** and **X**, v is a standardized Gaussian variable, and G(·) is a non-quadratic function. $\mathrm{G}(\cdot)=(\cdot)^4/4$ is adopted here. The fixed-point iterative scheme is used, then, to find a concrete representation of **W**.

After ICA mode separation, each individual component can be obtained, and the multimodal signals can be reconstructed through $\bar{\mathbf{X}}=\mathbf{W}^{-1}\bar{\mathbf{S}}$. In order to evaluate the reconstruction of the proposed algorithm, instead of the comparison of the TFR of the extracted components to the dispersion curves, the multimodal signals are also reconstructed through inverse STFT and compared with the original input signals. The similarity between two different signals is measured by the normalized cross-correlation coefficient:

$$r_{ij}=\textstyle\sum_k x_i(k)x_j(k)\Big/\sqrt{\sum_k x_i^2(k)\sum_k x_j^2(k)}. \tag{5}$$

The more similar the two signals are, the closer the value is to 1.

C. Simulation Settings

TABLE I. MATERIAL PARAMETERS OF THE STEEL PLATE

Parameters	h (mm)	ρ (kg/m^3)	c_T (m/s)	c_L (m/s)
Steel Plate	3	7932	3200	5960

A FDTD algorithm is used to simulate the propagation of Lamb waves in a steel plate. The relevant parameters [12] are presented in Table I, where h is the thickness of the plate, ρ is the density of steel, c_T and c_L correspond to the shear and longitudinal wave velocity respectively. The spatial step Δd is 50 µm, while the temporal step Δt is 3 ns.

A 5 cycle Gaussian amplitude-modulated sinusoidal signal is used as the excitation, whose center-frequency is 1 MHz, and -3 dB bandwidth is 0.28 MHz.

Axial transmission signal is applied in the simulation, *i.e.* probes are placed on the same side of the plate. The propagation distance is 200 mm. Mode selection can be achieved through adjusting the angle of incidence. To obtain combinations of the same set of modes at different weights, signals are excited at different angles (30°, 50°, and 60°) and received at the same location.

III. RESULTS

A. Short Time Fourier Transform Results

Figure 1 shows three independent measurements in the time-frequency domain with the incident angles being 30°, 50° and 60° individually. Different colors correspond to different energy levels, high in red and low in blue. Theoretical dispersion curves calculated through the Rayleigh-Lamb equation are plotted as a reference in black lines. Comparing with the theoretical dispersion curves, A0, S0, and S1 modes can be observed. The energy of each mode varies for different incident angles.

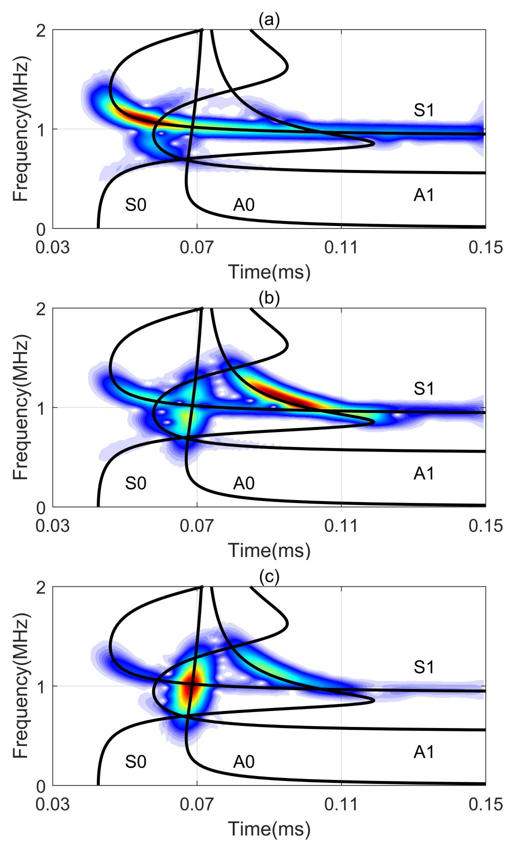

Fig. 1. Time-frequency representation of the received signals through STFT. Red and blue denote the most energetic and weak part, respectively. The black lines are theoretical dispersion curves. The emission angles are (a) 30°; (b) 50°; (c) 60°.

B. Multimodal Separation

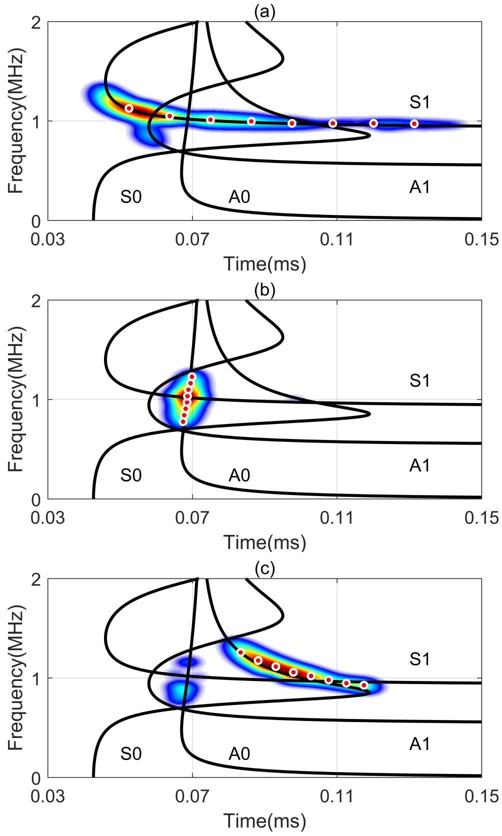

Fig. 2. Extracted individual time-frequency components of (a) S1; (b) A0; (c) S0. The energy ridges are marked with red dots with white border.

The separation result is depicted in Fig. 2. Mode separation is performed on the basis of the characteristics of the three received signals. The main components in Fig. 3 (a-c) are S1, A0 and S0 mode. After the mode extraction, the time-frequency energy ridge of each mode can further be extracted. The red dots with white border are the sampling points of their ridges. As shown in Fig. 3 (c), part of A0 mode energy leaks into the S1 mode components.

C. Temporal Multimodal Signal Reconstruction

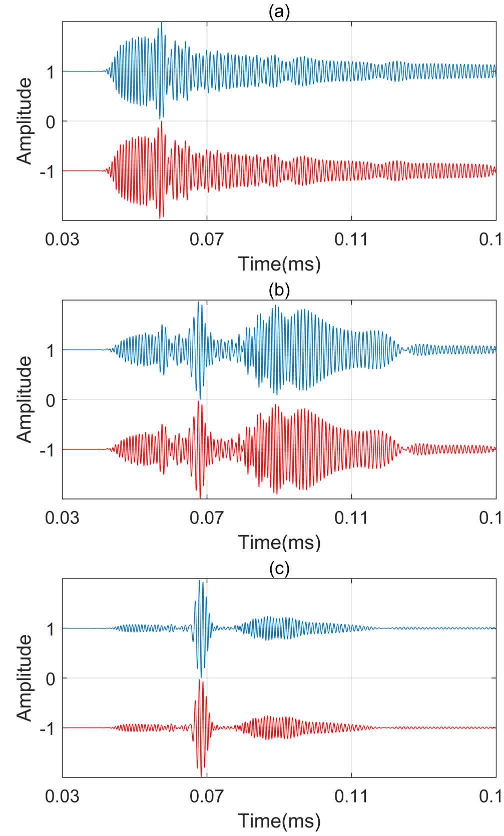

Fig. 3. The simulated and reconstructed signals. The simulated signals are presented in blue, with the reconstructed ones in red. Amplitude normalization is performed on each signal. The emission angles are (a) 30°; (b) 50°; (c) 60°.

As the received signals are considered as a linear superposition of multiple modes, the input signals can be reconstructed using the extracted components. Fig. 3 compares the simulated (the blue one) and reconstructed (the red one) signals. The amplitude of each signal is normalized. According to Eq. 5, the correlation coefficients of the three sets of signals are all 0.9998, which illustrates a good mode extraction and reconstruction.

D. Group Velocity Estimation

According to the energy ridges extracted in Fig. 2, the reaching time of each sampling dot can be acquired. As the distance between transmitter and receiver is known, frequency-dependent group velocity can be calculated directly. Fig. 4 exhibits the group velocity estimation results of different modes in the simulation. The average error rates of A0, S0 and S1 are 0.15%, 3.71% and 11.00% respectively.

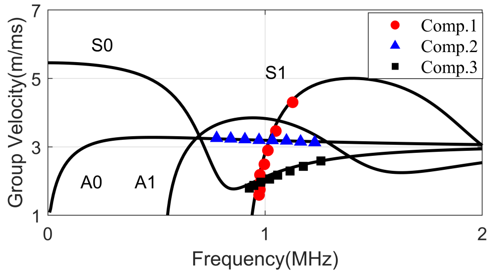

Fig. 4. Group velocity estimation results of separated components. The separated component 1-3 are S1, A0 and S0 in turn.

IV. Conclusion

In the study, a time-frequency ICA method was applied to separate the individual components from the overlapping multimode guided waves. Without the prior knowledge of waveguide, the proposed method can separate independent components in the time-frequency domain automatically. After mode separation, the group velocity of each mode was estimated. The simulated results show that estimates are consistent with the theoretical curves. It illustrates that the proposed time-frequency ICA method has a potential for the development of an automatic mode separation and group velocity estimation.

References

[1] Z. Su and L. Ye, "Identification of damage using Lamb waves: From fundamentals to applications," Springer Science and Business Media, vol. 48, 2009.

[2] K. Xu, D. Ta, and W. Wang, "Multiridge-based analysis for separating individual modes from multimodal guided wave signals in long bones," IEEE Transactions on Ultrasonics, Ferroelectrics, and Frequency Control, vol. 57, pp. 2480-2490, 2010.

[3] V. Kilappa, K. Xu, P. Moilanen, E. Heikkola, D. Ta, and J. Timonen, "Assessment of the fundamental flexural guided wave in cortical bone by an ultrasonic axial-transmission array transducer," Ultrasound in Medicine and Biology, vol. 39, pp. 1223-1232, 2013.

[4] A. B. Zoubi, S. Kim, D. O. Adams, and V. J. Mathews, "Lamb wave mode decomposition based on cross-Wigner-Ville distribution and its application to anomaly imaging for structural health monitoring," IEEE Transactions on Ultrasonics, Ferroelectrics, and Frequency Control, vol. 66, pp. 984-997, 2019.

[5] Y. Yang, Z. Peng, W. Zhang, G. Meng, and Z. Lang, "Dispersion analysis for broadband guided wave using generalized warblet transform," Journal of Sound and Vibration, vol. 367, pp. 22-36, 2016.

[6] Z. Zhang, K. Xu, D. Ta, and W. Wang, "Joint spectrogram segmentation and ridge-extraction method for separating multimodal guided waves in long bones," Science China Physics, Mechanics and Astronomy, vol. 56, pp. 1317-1323, 2013.

[7] Z. Liu, K. Xu, D. Li, D. Ta, and W. Wang, "Automatic mode extraction of ultrasonic guided waves using synchrosqueezed wavelet transform," Ultrasonics, vol. 99, pp. 105948, 2019.

[8] D. He, H. Cao, S. Wang, and X. Chen, "Time-reassigned synchrosqueezing transform: The algorithm and its applications in mechanical signal processing," Mechanical Systems and Signal Processing, vol. 117, pp. 255-279, 2019.

[9] T. N. H. T. Tran, L. H. Le, M. D. Sacchi, V. Nguyen, and E. H. M. Lou, "Multichannel filtering and reconstruction of ultrasonic guided wave fields using time intercept-slowness transform," The Journal of the Acoustical Society of America, vol. 136, pp. 248-259, 2014.

[10] T. N. H. T. Tran, K. C. T. Nguyen, M. D. Sacchi, and L. H. Le, "Imaging ultrasonic dispersive guided wave energy in long bones using linear radon transform," Ultrasound in Medicine and Biology, vol. 40, pp. 2715-2727, 2014.

[11] K. Xu, D. Ta, D. Cassereau, B. Hu, and W. Wang, "Multichannel processing for dispersion curves extraction of ultrasonic axial-transmission signals: Comparisons and case studies," The Journal of the Acoustical Society of America, vol. 140, pp. 1758-1770, 2016.

[12] K. Xu, D. Ta, P. Moilanen, and W. Wang, "Mode separation of Lamb waves based on dispersion compensation method," The Journal of the Acoustical Society of America, vol. 131, pp. 2714-2722, 2012.

[13] K. Xu, P. Laugier, and J. G. Minonzio, "Dispersive Radon transform," The Journal of the Acoustical Society of America, vol. 143, pp. 2729-2743, 2018.

[14] F. Gao, L. Zeng, J. Lin, and Z. Luo, "Mode separation in frequency–wavenumber domain through compressed sensing of far-field Lamb waves," Measurement Science and Technology, vol. 28, pp. 075004, 2017.

[15] A. K. H. Al-Ali, B. Senadji, and G. R. Naik, "Enhanced forensic speaker verification using multi-run ICA in the presence of environmental noise and reverberation conditions," 2017 IEEE International Conference on Signal and Image Processing Applications (ICSIPA). IEEE, pp. 174-179, 2017.

[16] Z. A. Acar, C. E. Acar, and S. Makeig, "Simultaneous head tissue conductivity and EEG source location estimation," NeuroImage, vol. 124, pp. 168-180, 2016.

[17] Z. Uddin, A. Ahmad, M. Iqbal, and M. Naeem, "Applications of independent component analysis in wireless communication systems," Wireless Personal Communications, vol. 83, pp. 2711-2737, 2015.

[18] M. Zvokelj, S. Zupan, and I. Prebil, "EEMD-based multiscale ICA method for slewing bearing fault detection and diagnosis," Journal of Sound and Vibration, vol. 370, pp. 394-423, 2016.

[19] L. Cohen, "Time-frequency distributions-a review," Proceedings of the IEEE, vol. 77, pp. 941-981, 1989.

[20] A. Hyvarinen, "Fast and robust fixed-point algorithms for independent component analysis," IEEE Transactions on Neural Networks, vol. 10, pp. 626-634, 1999.